Strong two-photon absorption of Mn-doped $CsPbCl_3$ perovskite nanocrystals

Tingchao He,[1] Junzi Li,[1] Can Ren,[1] Shuyu Xiao,[1] Yiwen Li,[2] Rui Chen,[2,a)] and Xiaodong Lin[1,a)]
[1]College of Physics and Energy, Shenzhen University, Shenzhen 518060, China
[2]Department of Electrical and Electronic Engineering, South University of Science and Technology of China, Shenzhen 518055, China

(Received 6 October 2017; accepted 5 November 2017; published online 21 November 2017)

Emerging $CsPbX_3$ (X = Cl, Br, and I) perovskite nanocrystals (NCs) have been demonstrated to be efficient emitters with a high fluorescence quantum yield, making these materials interesting for optical applications as well as for fundamental physics. Interestingly, doping with transition metal ions has been extensively explored as a way of introducing new optical, electronic, and magnetic properties, making perovskite NCs much more functional than their undoped counterparts. However, there have been no reports regarding the nonlinear optical properties of transition metal ion doped perovskite NCs. Herein, by using femtosecond-transient absorption spectroscopy, we have determined the one-photon linear absorption cross-section ($\sim 1.42 \times 10^{-14}$ cm^2) of Mn-doped $CsPbCl_3$ NCs ($\sim 11.7 \pm 1.8$ nm size, ~0.2% doping concentration, and ~600 nm emission wavelength). More importantly, their nonlinear optical properties—in particular, the two-photon absorption (TPA) and resultant emission—were investigated. Notably, the NCs exhibit wavelength-dependent TPA with a maximum value up to $\sim 3.18 \times 10^5$ GM at a wavelength of 720 nm. Our results indicate that Mn-doped $CsPbCl_3$ NCs show promise in nonlinear optical devices and multiphoton fluorescence lifetime imaging. *Published by AIP Publishing*. https://doi.org/10.1063/1.5008437

Semiconductor nanocrystals (NCs) have attracted much interest in both fundamental science and for applications, e.g., solar cells, light emitting diodes, lasers, or sensors.[1–3] By virtue of the 3D quantum confinement effect, NCs possess a size-tunable emission wavelength, well-separated delta function-like density of states, large optical oscillator strength, and nonlinear optical properties.[4–6] Ever since their emergence in 2014, perovskite NCs have aroused great attention in a short time and have become an important type of semiconductor NCs for various optoelectronic devices.[7] Numerous studies have already demonstrated that perovskite NCs might be promising in multiphoton bioimaging, if their sensitivity to moisture and polar solvents can be overcome.[8–11] It is a remarkable fact that Wei *et al.* reported superior water resistance and high stability of perovskite NCs by encapsulation in crosslinked polystyrene beads via a swelling–shrinking strategy, which ensures the suitability of their practical applications in multiphoton bioimaging.[12]

Currently, much effort has been expended on developing multiphoton excited fluorescence of perovskite NCs from an excitonic state with a lifetime in the order of a nanosecond.[8–11] However, such a short lifetime is disadvantageous for multiphoton bioimaging due to the strong autofluorescence from biological tissues. Therefore, there is still a great need to achieve new perovskite NCs working over long lifetimes in the order of microseconds to milliseconds (ms). Now, it appears that doping with transition metal ions into NCs, such as Mn^{2+} or Cu^{2+}, seems to be among the most favorable candidates for multiphoton fluorescent probes in biomedical applications.[13–15] Furthermore, doping of Mn^{2+} ions in semiconductor NCs is known to achieve emission wavelengths in the range of 585–600 nm, which is an additional advantage for bioimaging applications compared to their blue or green counterparts. More interestingly, doping of Mn^{2+} ions in NCs can also lead to longer lifetimes up to ms, enabling the temporal discrimination of the signal from the autofluorescence background.[16] Doping may also change multiphoton absorption (MPA) properties of NCs by forming defect levels in the bandgap.[17] Hence, the large MPA of Mn^{2+}-doped semiconductor NCs is appropriate for high-resolution cellular imaging and *in vivo* tumor-targeting imaging.[16] However, the role of Mn^{2+} defect levels in modifying the MPA properties of perovskite NCs has not been investigated. Here, we report on the nonlinear optical properties of Mn^{2+}-doped perovskite ($CsPbCl_3$:Mn) NCs using the Z-scan technique. Our results suggest that doping of Mn^{2+} ions in perovskite NCs can lead to large two-photon absorption (TPA) action cross-sections with fluorescence lifetimes in the order of ms, indicating their promising applications in multiphoton bioimaging, especially in multiphoton fluorescence lifetime imaging.

The detailed fabrication process of the $CsPbCl_3$:Mn NCs adopted here can be found in Ref. 18, and the Mn-doping concentration determined from elemental analysis is ~0.2% for $CsPbCl_3$. Figure 1(a) shows the linear absorption and fluorescence emission spectra of $CsPbCl_3$:Mn NCs in a hexane solution excited at 350 nm. It can be seen that $CsPbCl_3$:Mn NCs exhibit broad fluorescence attributed to the ligand field transition ($^4T_1 - {}^6A_1$) of Mn^{2+} ions at ~600 nm accompanied by the exciton emission of the host at 410 nm. The quantum yield (QY) of Mn fluorescence in Mn-doped $CsPbCl_3$ NCs was determined to be 30%. Their linear absorbance from wavelengths longer than ~410 nm is negligible. The transmission electron microscopy (TEM) image [Fig. 1(b)] illustrates the cubic shape of NCs with an edge length

a)Authors to whom correspondence should be addressed: chenr@sustc.edu.cn and linxd@szu.edu.cn

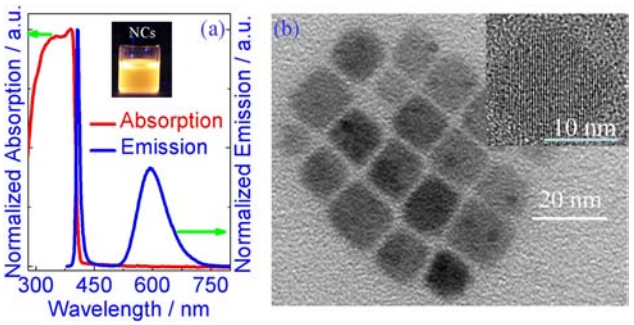

FIG. 1. (a) Absorption and emission spectra of as-prepared $CsPbCl_3$:Mn NCs. (b) TEM images of NCs. The inset in (a) shows the emission photograph of $CsPbCl_3$:Mn NCs dispersed in hexane, while the inset in (b) is the high-resolution TEM image.

of $\sim 11.7 \pm 1.8$ nm and with the high crystallinity of the host structure preserved in the $CsPbCl_3$:Mn NCs [inset of Fig. 1(b)]. Figure 2 shows the observed fluorescence decay curves at 410 nm and 600 nm, up to excitation at 350 nm. Exponential function fitting gives average lifetime values of 0.74 ns and 1.5 ms for emission from the host $CsPbCl_3$ NCs and Mn^{2+} defect state, respectively. Such a long lifetime for the emission at 600 nm, originating from the spin-forbidden ligand field transition of the doped Mn^{2+} ions, indicates that the $CsPbCl_3$:Mn NCs are promising candidates for fluorescence lifetime imaging.

The linear absorption cross-section (σ_{lin}) is an important factor that is used to determine the molar concentration and TPA cross-sections of semiconductor NCs. However, most σ_{lin} values of semiconductor NCs have been determined from Inductively Coupled Plasma-Atomic Emission Spectrometry (ICP-AES), which is very challenging due to their size and composition inhomogeneity and the disturbance from the indispensable surface ligands. As a result, the reported TPA cross-sections varied by up to one order of magnitude among

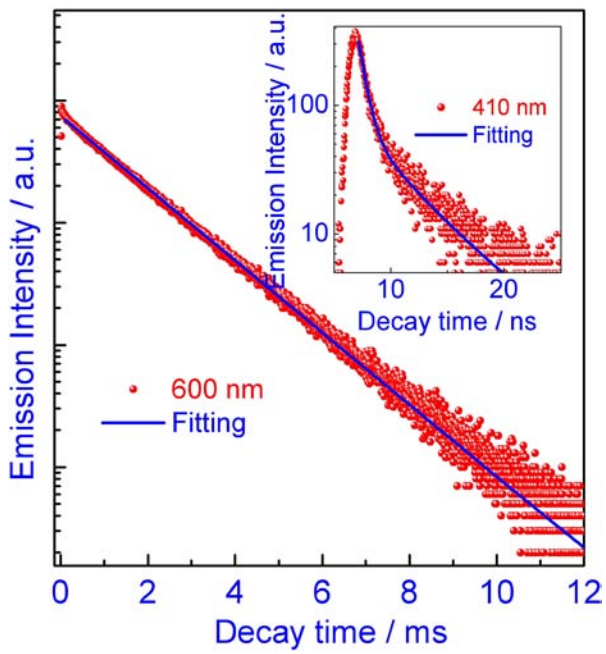

FIG. 2. Time-dependent Mn^{2+} fluorescence intensity at 600 nm from $CsPbCl_3$:Mn NCs. The inset is the time-dependent exciton fluorescence of the host at 410 nm.

semiconductor NCs even within the same class.[6,9] Here, we attempt to estimate the σ_{lin} value of $CsPbCl_3$:Mn NCs from the excitation intensity-dependent one-photon induced ground state bleaching (GSB) signals by using femtosecond-transient absorption (fs-TA) spectroscopy.[19] The pump pulses at 350 nm were generated by an optical parametric amplifier (Topas, Light Conversion). The probe pulses in the wavelengths between 350 and 800 nm were achieved by supercontinuum generation from a thin CaF_2 plate. The excitation intensity-dependent fs-TA kinetics for the wavelength of the maximum GSB of $CsPbCl_3$:Mn NCs were probed [Fig. 3(a)]. After fast Auger recombination within the initial hundreds of picoseconds, NCs will contain only a single exciton in the following time period, which is demonstrated by the parallel decay lines from all the excitation intensities after a long time delay (>0.5 ns). The GSB signal amplitude at different excitation intensities varies according to the following equation:

$$-A(I/I_0) = -A_{max}[1 - e^{-(I/I_0)\cdot\sigma\cdot I_0}], \quad (1)$$

where $A(I/I_0)$ denotes the GSB signal amplitude of $CsPbCl_3$:Mn NCs after a long time delay as a function of excitation intensity, and I_0 is the minimum excitation intensity used in the fs-TA experiment.[19] As shown in Fig. 3(b), the excitation intensity-dependent GSB signal amplitude with a delay time of 1 ns could be well fitted with Eq. (1), from which the value of σ_{lin} is extracted to be $\sim 1.42 \times 10^{-14}$ cm^2. Correspondingly, the molar distinction coefficient of $CsPbCl_3$:Mn NCs was determined to be 3.7×10^6 L cm^{-1} mol^{-1} at 350 nm.

Subsequently, the TPA properties of $CsPbCl_3$:Mn NCs were investigated. Upon excitation with femtosecond pulses

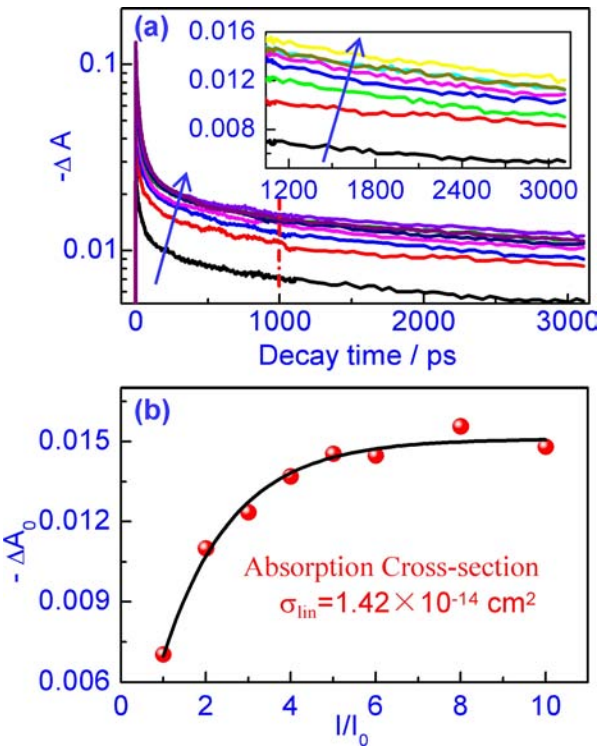

FIG. 3. (a) Excitation intensity-dependent decay traces of $CsPbCl_3$:Mn NCs, resolving the Auger recombination at high excitation intensities. (b) GSB signal amplitude at a time delay of 1 ns as a function of excitation intensity. The curve is the best fitting line based on Eq. (1).

at 720 nm, the $CsPbCl_3$:Mn NCs emitted red fluorescence from hexane solution (inset of Fig. 4, with the excitation light blocked by a low-pass filter). Since linear absorption beyond 410 nm was absent for the studied $CsPbCl_3$:Mn NCs, the observed fluorescence was thus plausibly attributed to TPA. Such a mechanism was further confirmed through measurements of the power-dependent fluorescence intensity (Fig. 4). The inset of Fig. 4 depicts the logarithmic plot of the emission integral versus the pumped power with a slope of around 2, suggesting a TPA mechanism. It was interesting to note that the emission from the host was stronger than that from the Mn^{2+} defect state excited at 350 nm but was completely quenched when excited at 720 nm, indicating a more efficient two-photon excited energy transfer compared to the case of one-photon excitation.[20] The different spectral behaviors under one- and two-photon excitation arise because the TPA cross-sections of the donor (the host) and the acceptor (Mn^{2+} ions) were different from those under one-photon excitation.[21]

The TPA cross-sections of $CsPbCl_3$:Mn NCs were determined by the open-aperture Z-scan technique introduced by Sheik-Bahae *et al.*,[22] and the corresponding TPA spectra calculated on the basis of the Z-scan technique are presented in Fig. 5. Larger values for the TPA cross-section were observed in the short wavelength range of 680 to 730 nm, peaking at 720 nm with $\sigma_2 = 3.18 \times 10^5$ GM (1 GM = 10^{-50} cm^4 s^{-1} $photon^{-1}$). Based on the analysis of the σ_2 values for wavelength dispersion, we noticed that the maximum TPA cross-section appears to be significantly blue-shifted with respect to the first exciton peak in the linear absorption spectra multiplied by a factor of two. Shifting of the TPA maxima towards higher energy was concluded to be a consequence of different selection rules for one- and two-photon transitions.[23] The two-photon excitation action cross-section (σ_2·QY) of per individual $CsPbCl_3$:Mn NC, the parameter relevant for nonlinear bioimaging, was equal to 95 400 GM

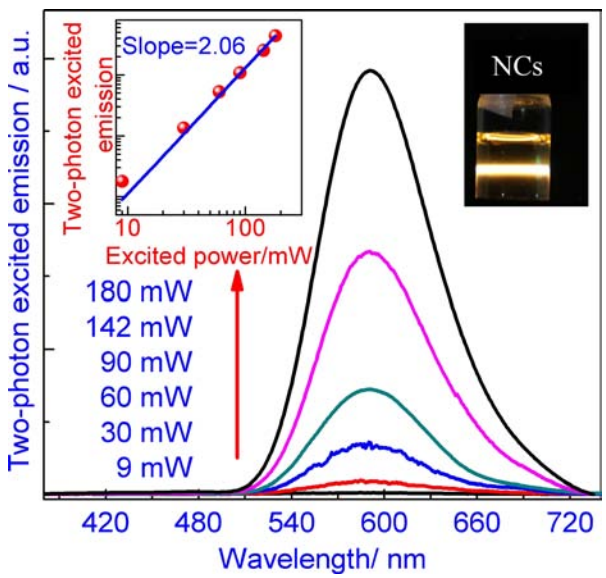

FIG. 4. Excitation intensity-dependent emission spectra from $CsPbCl_3$:Mn NCs at 720 nm. The right inset shows the emission photograph of the NCs solution in which a low-pass filter (<700 nm) was used to block the excitation light, while the left inset shows a plot of integrated emission intensity as a function of excitation intensity.

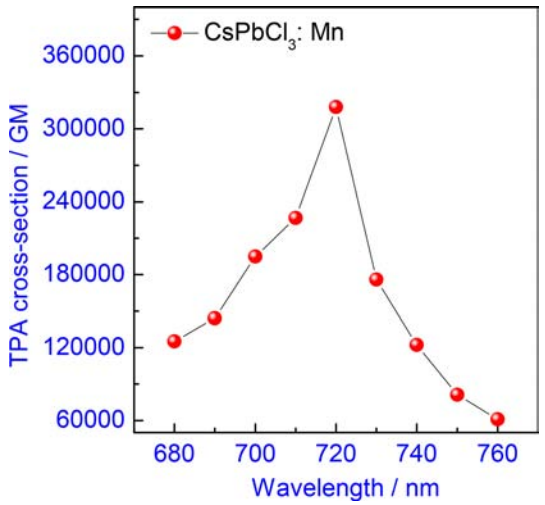

FIG. 5. Wavelength dispersion of TPA cross-section for per individual $CsPbCl_3$:Mn NC, measured by the Z-scan technique. The solid line is added as a guidance to the eye.

at 720 nm. This value is 1–2 orders of magnitude higher than the values of two-photon brightness for -NH_2 modified graphene oxide conjugates (~16412 GM),[24] colloidal InP/ZnS core-shell NCs (~2418 GM),[25] stilbene chromophore (~380 GM),[26] and diketopyrrolopyrrole derivatives (~1011 GM).[27] From the previous report, it is known that TPA cross-sections correlate strongly with NC size and follow a power-law dependence on NC size with exponent ~3.[19] Compared to similarly sized pure $CsPbBr_3$ NCs with green emission (~1.2×10^5 GM),[5] the $CsPbCl_3$:Mn NCs even exhibit comparable TPA. Additionally, when using the light power intensity of 2.4 GW/cm^2, the TPA signal of the blue emissive host ($CsPbCl_3$) NCs is submerged in noise while the signal of $CsPbCl_3$:Mn NCs can be easily detected. It can be concluded that the upper limit of TPA for $CsPbCl_3$ NCs should be less than 12000 GM. Such a large TPA of $CsPbCl_3$:Mn NCs indicates that doping with Mn^{2+} ions can effectively modify their TPA due to the sufficiently strong exchange coupling between the charge carriers of the host and dopant d electrons mediating the energy transfer and considerable enhancement in the density of states of the defect levels.[13,17,21,28] It is well known that different Mn-doping concentrations may result in distinct optical properties of semiconductor NCs. The relevant experimental investigations are not available in this work and are now in progress. Even so, we may find conclusions from previous reports.[17,29] The increase in the doping concentration in a certain range can help to further decrease the local field correction factor, which will induce enhancement in the TPA of $CsPbCl_3$:Mn NCs.[29] Furthermore, the lifetime of the ~600 nm fluorescence of $CsPbCl_3$:Mn NCs should decrease with the increase in the doping concentration, as a result of the increase in the oscillator strength.[17]

In conclusion, we have determined the linear absorption cross-section of emerging all-inorganic $CsPbCl_3$:Mn NCs using fs-TA spectroscopy. More importantly, based on the obtained experimental results, we have investigated their TPA properties by using the Z-scan technique. Considering the extremely strong two-photon brightness and ultralong fluorescence lifetime from the Mn^{2+} defect state of $CsPbCl_3$:Mn

NCs, the reported TPA properties of these NCs can effectively widen their possible applications in bioimaging, especially in fluorescence lifetime imaging.

We thank the National Natural Science Foundation of China (NSFC Grant Nos. 11404219, 11404161, and 21402124), the Natural Science Foundation of Guangdong Province (Grant No. 2014A030313552), and the Shenzhen Basic Research Project of Science and Technology (Grant Nos. JCYJ2015032414171163, JCYJ20150930160634263, and KQTD2015071710313656).

[1]L. Jing, S. V. Kershaw, Y. Li, X. Huang, Y. Li, A. L. Rogach, and M. Gao, Chem. Rev. **116**, 10623 (2016).
[2]J. Song, J. Li, X. Li, L. Xu, Y. Dong, and H. Zeng, Adv. Mater. **27**, 7162 (2015).
[3]G. Li, Z. Tan, D. Di, M. L. Lai, L. Jiang, J. Lim, R. H. Friend, and N. C. Greenham, Nano Lett. **15**, 2640 (2015).
[4]Y. Wang, K. S. Leck, V. D. Ta, R. Chen, V. Nalla, Y. Gao, T. He, H. V. Demir, and H. Sun, Adv. Mater. **27**, 169 (2015).
[5]Y. Wang, V. Duong Ta, K. S. Leck, B. H. I. Tan, Z. Wang, T. He, C. Ohl, H. V. Demir, and H. Sun, Nano Lett. **17**, 2640 (2017).
[6]Y. Wang, X. Li, X. Zhao, L. Xiao, H. Zeng, and H. Sun, Nano Lett. **16**, 448 (2016).
[7]L. Protesescu, S. Yakunin, M. I. Bodnarchuk, F. Krieg, R. Caputo, C. H. Hendon, R. X. Yang, A. Walsh, and M. V. Kovalenko, Nano Lett. **15**, 3692 (2015).
[8]W. Chen, S. Bhaumik, S. A. Veldhuis, G. Xing, Q. Xu, M. Gratze, S. Mhaisalkar, N. Mathews, and T. C. Sum, Nat. Commun. **8**, 15198 (2017).
[9]Y. Xu, Q. Chen, C. Zhang, R. Wang, H. Wu, X. Zhang, G. Xing, W. W. Yu, X. Wang, Y. Zhang, and M. Xiao, J. Am. Chem. Soc. **138**, 3761 (2016).
[10]K. Wei, Z. Xu, R. Chen, X. Zheng, X. Cheng, and T. Jiang, Opt. Lett. **41**, 3821 (2016).
[11]W.-G. Lu, C. Chen, D. Han, L. Yao, J. Han, H. Zhong, and Y. Wang, Adv. Opt. Mater. **4**, 1732 (2016).
[12]Y. Wei, X. R. Deng, Z. X. Xie, X. C. Cai, S. S. Liang, P. A. Ma, Z. Y. Hou, Z. Y. Cheng, and J. Lin, Adv. Funct. Mater. **27**, 1703535 (2017).
[13]M. Chattopadhyay, P. Kumbhakar, R. Sarkar, and A. K. Mitra, Appl. Phys. Lett. **95**, 163115 (2009).
[14]C. Gan, M. Xiao, D. Battaglia, N. Pradhan, and X. Peng, Appl. Phys. Lett. **91**, 201103 (2007).
[15]X. Peng, J. Li, Y. Yang, H. Gong, F. Nan, L. Zhou, X. Yu, Z. Hao, and Q. Wang, J. Appl. Phys. **112**, 074305 (2012).
[16]N. G. Horton, K. Wang, D. Kobat1, C. G. Clark, F. W. Wise, C. B. Schaffer, and C. Xu, Nat. Photonics **7**, 205 (2013).
[17]R. Subha, V. Nalla, J. H. Yu, S. W. Jun, K. Shin, T. Hyeon, C. Vijayan, and W. Ji, J. Phys. Chem. C **117**, 20905 (2013).
[18]D. Parobek, B. J. Roman, Y. Dong, H. Jin, E. Lee, M. Sheldon, and D. H. Son, Nano Lett. **16**, 7376 (2016).
[19]J. Chen, K. Žídek, P. Chábera, D. Liu, P. Cheng, L. Nuuttila, M. J. Al-Marri, H. Lehtivuori, M. E. Messing, K. Han, K. Zheng, and T. Pullerits, J. Phys. Chem. Lett. **8**, 2316 (2017).
[20]T. He, R. Chen, Z. B. Lim, D. Rajwar, L. Ma, Y. Wang, Y. Gao, A. C. Grimsdale, and H. Sun, Adv. Opt. Mater. **2**, 40 (2014).
[21]T. He, Y. Gao, R. Chen, L. Ma, D. Rajwar, Y. Wang, A. C. Grimsdale, and H. Sun, Macromolecules **47**, 1316 (2014).
[22]M. Sheik-Bahae, A. A. Said, T. H. Wei, D. J. Hagan, and E. W. Van Stryland, IEEE J. Quantum Electron. **26**, 760 (1990).
[23]D. Wawrzyńczyka, J. Mater. Chem. C **5**, 1724 (2017).
[24]R. Gui, H. Jin, Z. Wang, and L. Tan, Coord. Chem. Rev. **338**, 141 (2017).
[25]Y. Wang, X. Yang, T. C. He, Y. Gao, H. V. Demir, X. W. Sun, and H. D. Sun, Appl. Phys. Lett. **102**, 021917 (2013).
[26]T. He, Y. Wang, X. Tian, Y. Gao, X. Zhao, A. C. Grimsdale, X. Lin, and H. Sun, Appl. Phys. Lett. **108**, 011901 (2016).
[27]T. He, Y. Gao, S. Sreejith, X. Tian, L. Liu, Y. Wang, H. Joshi, S. Z. F. Phua, S. Yao, X. Lin, Y. Zhao, A. C. Grimsdale, and H. Sun, Adv. Opt. Mater. **4**, 746 (2016).
[28]R. Subha, V. Nalla, X. Feng, C. Vijayan, and W. Ji, AIP Conf. Proc. **1620**, 401 (2014).
[29]D. More, C. Rajesh, A. D. Lad, G. R. Kumar, and S. Mahamuni, Opt. Commun. **283**, 2150 (2010).